Sensors position optimization for monitoring the convergence of radioactive waste storage tunnel

Elodie Chapoulade, Aurélie Talon, Alaa Chateauneuf, Pierre Breul, Guillaume Hermand, Marc Leconte

Sensors position optimization for monitoring the convergence of radioactive waste storage tunnel

*Chapoulade Elodie [a, b], Talon Aurélie [a *], Chateauneuf Alaa [a], Breul Pierre [a], Hermand Guillaume [b], Leconte Marc [b]*

[a] Université Clermont Auvergne, CNRS, Institut Pascal UMR 6602 – 63171 Aubière, France
[b] ANDRA, 1/7 rue Jean Monnet, Parc de la Croix-Blanche – 92298 Châtenay-Malabry, France

Abstract

In the Cigéo project for deep geological of radioactive waste, the project manager has to follow the convergence of tunnel (cells) cross-section built at 490 m depth. This convergence is due to the mechanical pressure in the rock layer. Vibrating Wire Extensometers (VWE) are used to measure the strain at their locations. Our objective is to optimize the location of sensors to estimate the horizontal stress due to strain observations. This issue is solved using an inverse problem, which first requires the creation of a direct model that represents the behaviour of a cross-section. From rock data measured on site, thanks to an underground demonstrator, a numerical model is developed to generate a strain database for different VWE locations with different rock stresses and rigidities. The theoretical orientation of the sensors is orthoradial, but they can have angle and intrinsic errors. Considering various types of uncertainties, an inverse model based on Bayesian approach is developed to calculate the probability distribution of stresses. The last step is to use a genetic algorithm to determine the optimal sensor distribution. The best sensor placements is found to be near the kidneys, i.e. at more or less 45° around 0° and 180°.

Keywords: Monitoring, Optimization, Genetic Algorithm, Radioactive waste storage tunnel.

* Corresponding author at: Polytech Clermont-Ferrand, Campus Universitaire Des Cézeaux, 2 avenue Blaise Pascal, 63178 Aubière, France.
Email address: aurelie.talon@uca.fr

1. Introduction

Today, many countries using nuclear energy are faced to the problem of managing the waste and according to different studies like NAGRA 1983 (National Cooperative for the Disposal of Radioactive Waste) or Yucca Mountain Project 1984 (Alexander and McKinley 2011, CoRWM 2018; Department of Business, Energy & Industrial Strategy 2018), the best alternative seems to be deep geological disposal. In France, the deep geological industrial storage center Cigéo project, when approved, will be a nuclear installation for radioactive waste. This project aims at storing in tunnels located at 490m deep in a clay layer, high activity (HA) and average long life activity (MAVL) radioactive waste. The project constraints are mainly the reversibility and the progressive storage of waste packages, over 100 years. For this reasons, it is necessary to monitor the structural strains by performing instrumentation and optimizing the location of the sensors in order to measure the convergence of cells in which the radioactive waste will be stored. Due to their robustness and the feedback of more than 80 years (Rosin-Corre and al. 2012), the Vibrating Wire Extensometer (VWE) have been preferred over the other sensors for monitoring the storage cells.

All structure degrade over time and preoccupations about their conditions have prompted numerous studies on damage detection. This falls within this framework of structural health monitoring (SHM). Usually, the damage identification methods are classified on four levels (Rytter 1993) according to their finesse of analysis:

- Methods detecting the presence of damage in the structure. These methods are based on either the direct measurement of a parameter, using sensors such as strain or stress gauges, vibrating wire (Kudva and al. 1992; Dinis da Gama 2004; Guan and Karbhari 2008; Zhou and Wu 2017) or non-invasive methods such as scans, electrical or ultrasonic measurements (Sbartaï and al. 2012; Ravi and al. 2016). Another possibility consists in studying the behaviour of structures under controlled stress (Lifshitz and Rotem 1969; Spillman and al. 1993; Doebling and al. 1996; Guratzsch and Mahadevan 2006; Guratzsch 2007; Guan and Karbhari 2008; Abdo 2012; Goi and Kim 2017). In most cases, damage detection is carried out using regularly distributed sensors. The detection is done at an instant *t* and the

structures are never inspected as a whole. Uncertainties are rarely considered in these works.

- The next two levels of damage detection are often treated together. These are the methods for locating and quantifying the severity of the damage. In the 1990s, using neural networks has grown to estimate the extent and the location of damages in structures (Bishop 1994; Spillman et al. 1993; Rhim and Lee 1995; Seleemah and al. 2012). Using sensor measurements, this method can predict the location of the damaged area without error (Kudva and al. 1992; Guratzsch and Mahadevan 2006; Guratzsch 2007), but it is not very robust to allow the determination of the size of defects. Moreover, the works carried out on damage detection are essentially based on a regular sensor distribution within the structure.
- Method for forecasting the residual life of the structure. Its objective is to estimate the operating time before the appearance of the damage or the residual life as well as the risk of existence or subsequent appearance of one or more damage (Ihn 2006). Although this information is what scientists are looking for, very few applications are available.

Cigeo project being based on the storage reversibility of radioactive waste, the aim of this project is to verify that cells strains do not exceed the clearance handling of the packages. These strains are mainly due to the soil stresses imposed on the cells. The objective of optimizing sensor locations making it possible to measure these strains can be akin to locating the most significant damage within a cell cross-section. So, this study focuses on the second and the third level of the damage identification methods with the objective of optimizing the location of strain sensors.

The objective being to find the stress at the origin of a strain, it is an inverse problem. A problem is said to be inverse when it allows the causes to be determined from the effects. To distinguish these solutions from each other, it is essential to have additional information. Solving an inverse problem consists in reformulating, in the form of the minimization of an error function between the real measures and the measures of the direct problem. Among various method for solving an inverse problem, there is in particular the Bayesian inference which takes into account uncertainties and errors due to the measurement system. Several researchers have

used Bayesian approach for monitoring the structural health. The data measured from the structure allows identifying the stiffness parameters of the structure (Vanik and al. 2000) or to estimate the location (Yan and al. 2016), the size, the direction and the depth of damages (Zhang and Yang 2012).

Among the two main optimization methods (continuous and combinational methods), given the finite number of solutions for the considered problem, optimization is combinational. But, in our case, one of the major problem with methods for optimizing the sensor locations in structures is that the number of potential locations will cause a combinatorial explosion, i.e. it exponentially increases with the number of variables (Dreyfus and al. 2002). Under these conditions, researchers use heuristics, which provide reliable solutions whose optimal character can be guaranteed, within a reasonable calculation time.

The metaheuristics (Ausiello and al. 1995; Hao and al. 1999) which can be seen as an extension of the concept of heuristics are generic methods allowing the performance of heuristics to be improved by overcoming their main weaknesses, in particular through mechanisms allowing them to extract themselves from local optimums (Segretier 2013). The metaheuristics are actually very common and efficient for optimising the number and locations of the sensors as it has been shown in different works (Moslem and Nafaspour 2002; Greistorfer 2003; Perry and al. 2006; Guratzsch 2007; Preis and Ostfeld 2008; Koh and Perry 2010; Aval and Razak 2012; Domingo-Perez and al. 2016; Zhou and Wu 2017; Wrigley and al. 2019).

Among the different metaheuristics algorithms (Simulated annealing algorithm (SA) (Černỳ 1985), Tabu search algorithm (TS) (Glover 1986), Ant Colony Optimization algorithm (ACO) (Dorigo and Di Caro 1999), Genetic Algorithm (GA) (Goldberg and Holland 1988), Particle Swarm Optimization (PSO) (Kennedy and Eberhart 1995)), the choice has to be done on the basis of different criteria: ease to implement, flexibility, the parameters number and their difficulty to adjust, computation time.

Some researchers (Aval and Razak 2012) indicated that GA and PSO were the two most used techniques to solve an optimization problem. Others researchers (Hammouche and al. 2010; Khoshahval and al. 2011) compared different algorithms

with each other and showed that GA and PSO converge faster, are more robust and more precise than the other algorithms. Finally, the GA converge in less generations but have a longer execution time than PSO. The number of parameters to be adjusted being lower in GA, this gives less uncertainties about the method.

If several works showed the efficiency of these algorithms, most of them do not consider uncertainties (Perry and al. 2006; Koh and Perry 2010) and work only on data from numerical simulations. Moreover, the influence of the number of sensors is rarely evaluated.

This paper presents a method for optimizing the VWE sensor locations and number within a storage cell cross-section based an inverse Bayesian model and a GA algorithm and taking into account various uncertainties (soil Young's modulus, sensor intrinsic error and sensor location error). In a first part, the proposed optimization method is presented. Then the model and the choice of the input parameters are discussed. The third part deals with the results of inverse model and the influence of the sensors number and location and finally the results of the optimization of the number and locations of the sensor are presented.

2. Proposed optimization method

The methodology for observing and monitoring storage cells must address both the knowledge necessary for the storage exploitation, and the reversiblility management. They also contribute to safety analyses in operation and after closure. For risk management related to cell strain, this research work must define the optimal instrumentation. The optimization steps are (Fig. 1):

- From the characteristics of the surrounding soil noted on the site and uncertainties considered, a finite element model representing a cell cross-section was developed in order to create a database of strains.
- From the VWE strains observations noted on the site and from previously created database, an inverse Bayesian model will estimate the horizontal stress at the origin of the observed strains.

- For different number and/or placement of VWE on a cell cross-section, a fitness function will allow the results of the inverse model to be compared with each other. A GA will create new combinations of VWE placement for a given number of sensors and using the fitness function will ultimately give the optimal solution to estimate the horizontal stress.

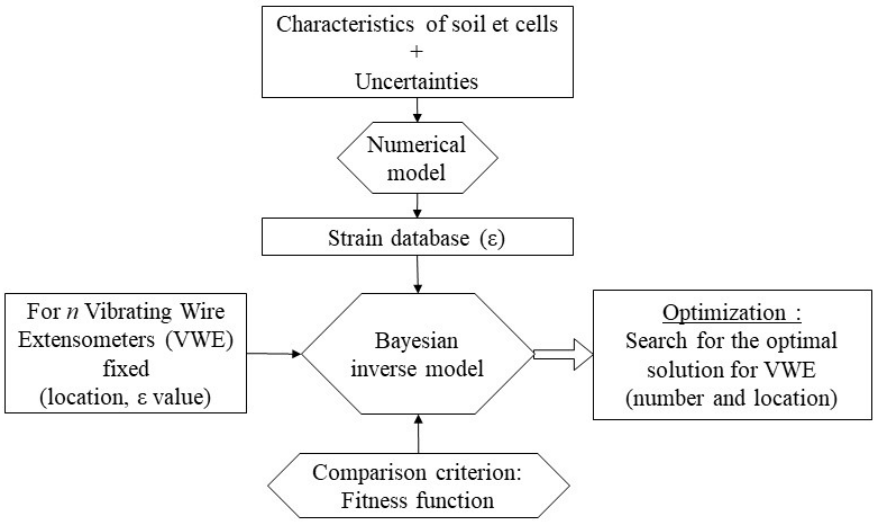

Fig. 1. Global methodology to answer the problem of optimizing the number and location of sensors in a tunnel.

2.1 Modelling tunnel cross-section

The tunnel cross-section has a thickness of 0.30 m. The outer diameter is of 5 m and the surrounding soil is an anisotropic clay layer. When digging the tunnel, the soil is damaged to a certain depth (about 3 m) and then anchor bolts compensate the resistance lost in this area. For modelling simplification, the combination of damaged soil and anchor bolts is considered equivalent to healthy soil. In the concrete thickness of the tunnels, VWE sensors are placed in cages. In each cage, there are two sensors: one orthoradial intrados and one orthoradial extrados.

A finite element model FEM representing a tunnel cross-section has been developed using the finite element code Cast3M (Cast3M 2003). This model is developed to calculate the strain in the tunnel at the possible sensor locations. The

tunnel cross-section is modelled by quadratic elements with linear elastic behaviour. The surrounding soil is represented by Winkler springs as shown in Fig. 2, and has a random rigidity principally due to the variability of the Young's modulus. Horizontal and vertical stresses are applied on the tunnel. So these initial conditions are the random rigidity of springs and the stress value. All the VWE locations allow us to build a database whatever the stress applied to the tunnel.

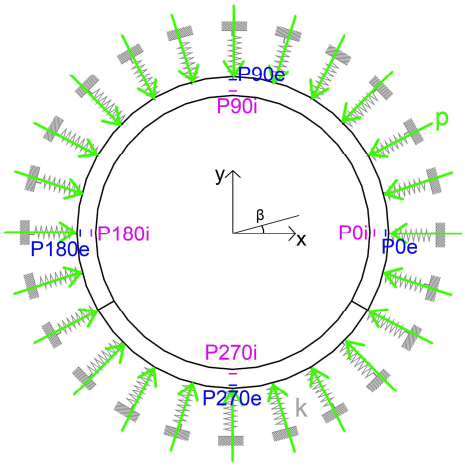

Fig. 2. Finite element model of the tunnel cross-section. Each mesh is 3 cm * 5.5 cm.

In Fig. 2, the VWE are symbolized by lines and their names are noted *P*"*0*"*e*" with "*0*" the angle β of the sensor location with respect to the horizontal and "*e*" or "*i*" for respectively the extrados or intrados location. The surrounding soil is modelled using 280 springs with stiffness *k*. The stress is converted into punctual equivalent point stress *p* before being modelled.

2.2 Parameters

For the structure, the concrete parameters are the Young's modulus E_c of 39.1 GPa and the Poisson's ratio v_c of 0.25. These values come from the underground laboratory (set of tunnels already built in order to test construction techniques and reliability of monitoring tools).

The surrounding soil is represented by springs, with variable stiffness k depending on the clay Young's modulus E_{soil} and Poisson's ratio v_{soil}. Respectively, modulus E_{soil} is arbitrarily supposed between 3 GPa and 9 GPa and v_{soil} is equal to 0.29. These values are drawn from soil studies in the clay layer of the project (Andra 2005 and internal Andra reports).

The rigidity of the springs is defined according to Winkler model (Jacob 2006):

$$\boldsymbol{k_s = \frac{E_{soil}}{R_m(1-v_{soil}^2)}} \quad (1)$$

With Rm the medium radius of the springs. The calculation of the spring rigidity ks is multiplied by the length of the extrados contour taken up by each spring. In Fig. 3, k_{moy} corresponds to k_s with E_{soil} the Young's modulus mean, i.e. 6 GPa.

Considering eight normal centred laws Δ_1 to Δ_8. Each one corresponds to the variation of the Young's modulus mean, E_{soil}, of 6 GPa with extreme values at ± 3 GPa. These eight laws allow us calculate eight rigidity soil distributions k_i (Eq. 1) and can thus be applied to eight springs of the numerical model (Fig. 3). If a spring is placed at each node of the outer contour of the modelled cell, the eight calculated stiffness distributions are associated with eight springs placed every 45° (starting from 0°). The choice of a new law every 45° is made to allow a significant variability on a section and to prevent the symmetry in the measure of strains. Between two springs separated by 45°, the evolution of the rigidity k_i is linear and its calculation, for each intermediate spring, corresponds to an interpolation between two values at 45°. The linear simplification comes from the fact that soil variability is modelled by a random field whose values are self-correlated. The vertical symmetry of the problem cannot be used to improve the efficiency of the optimization algorithm because the stiffness k of each springs of the FEM can be different. So neither symmetry is possible.

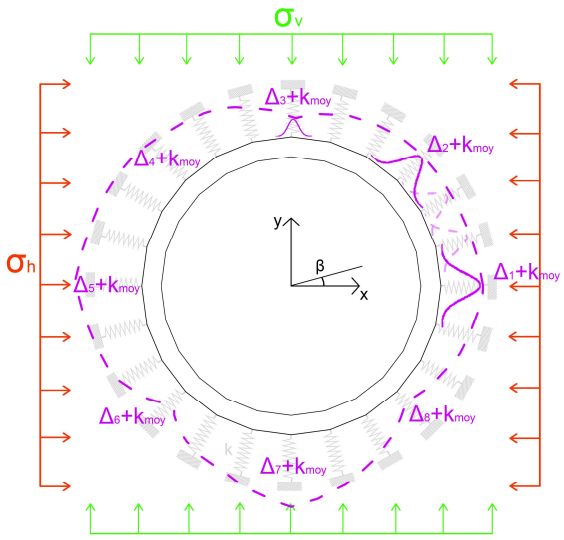

Fig. 3. Linear evolution of the rigidity between two normal laws (Δ_1 to Δ_8).

The surrounding soil of the tunnels, is anisotropic with a constant vertical stress equal to 12.7 MPa. The horizontal stress is constant on one section but vary from one section to another between 12 and 18 MPa. For the generation of the strain database, intrados and extrados strains are recorded at each degree of the cross-section for seven loading cases σ_h between 12 MPa and 18 MPa. The output of the analysis is the distribution of strain for each possible position of the sensors. Input and output parameters of the numerical model are synthetized in Table 1.

Table 1

Input and output parameters of the numerical model.

Input parameters				**Output parameters**	
Structure		**Surrounding soil**			
Diameter	5 m	σ_h	12 MPa to 18 MPa	**Intrados strain at each degree (β)**	ε_{int}
Thickness	0.3 m	σ_v	12.7 MPa		
E_c	39.1 GPa	E_{soil}	3 GPa to 9 GPa	**Extrados strain at each degree (β)**	ε_{ext}
ν_c	0.25	ν_{soil}	0.29		

In the real tunnel, the VWE orientation may vary due to the implementation phase and concrete casting. This uncertainty on the angle θ of the VWE position compared to its theoretical orthoradial position is taken into account. This uncertainty is considered by a normal distribution with $\pm 20°$ of sensor orientation error corresponding to ± 3 standard deviations (Fig. 4). These errors are considered as the lower and upper bounds of the confidence interval defined by six standard deviations; i.e. probability of $3*10^{-3}$ to have greater errors than these bounds. In addition, the sensor intrinsic error of 1.75 % (Mei 2016) due to its resonance is also taken into account.

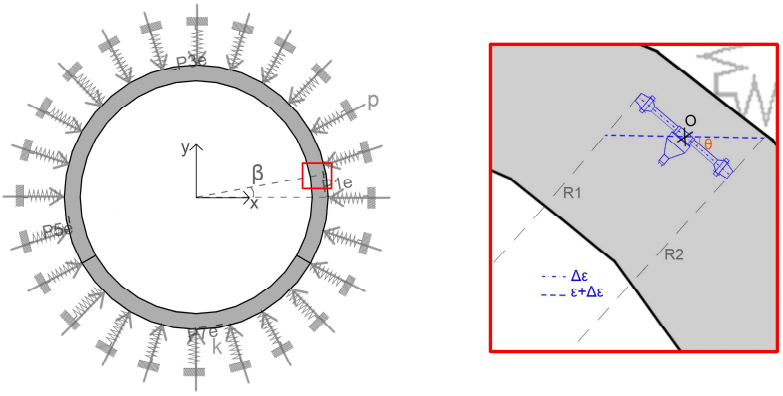

Fig. 4. Uncertainty about the orthoradial theoretical position of the VWE.

At one VWE location (Fig. 4 - red frame), the theoretical VWE position is centred in O. $\Delta\varepsilon$ is the length variation of the wire at the theoretical position and $\varepsilon + \Delta\varepsilon$ is the length variation of the wire with the uncertainty θ.

2.3 *Database*

As presented in Table 2, the model allows generating a strain database for each VWE position for a variation of stress between 12 MPa and 18 MPa. From a case of constant loading $\sigma_{h\ target}$ and normal distribution of stiffness k_i, the FEM results give normal laws of local strain at the VWE position. The sensor *P0e* at 0° extrados (Fig. 2) provides the results presented in Fig. 5.

Table 2

Contents of the strain database ε for each degree β, each intrados i and extrados e location and each horizontal stress σ_h (Fig. 2).

$\sigma_{h\ target}$ [MPa]	12							13			14	15	16	17	18		
β [°]	0	0	1	1	…	359	359	0	…	359	…	…	…	…	0	…	359
Intrados (*i*) Extrados (*e*)	e	i	e	i	…	e	i	e	…	i	…		…		e	…	i
Values stem from normal strain laws ε	ε_1	…				ε_1				…							
	…					…											
	ε_{500}					ε_{500}											

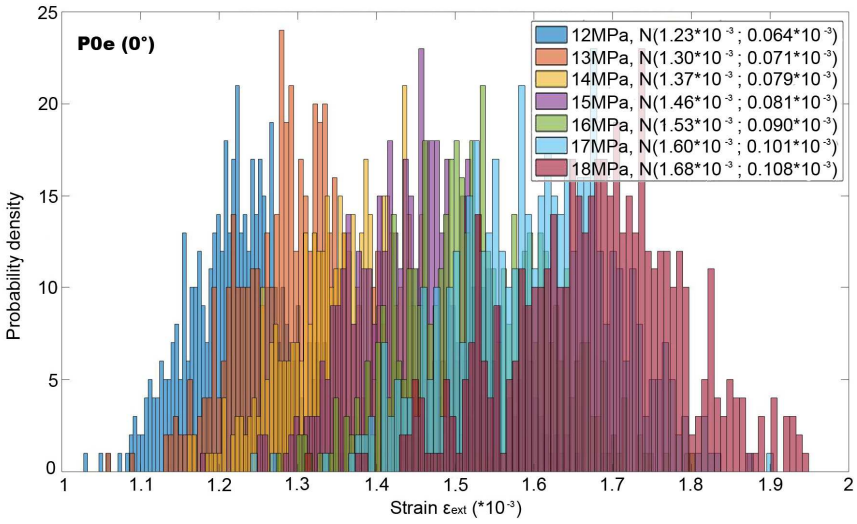

Fig. 5. Normal laws of strain for extrados VWE ε_{ext} at 0° for each horizontal stresses $\sigma_{h\ target}$ between 12 MPa to 18 MPa.

3. Horizontal stress at the origin of measured strains

In Cigéo project, the strains measured at VWE location are the only known measurements. The model provides all these strains at all VWE locations for all stresses levels. In the reality, one sensor gives one strain observation $\varepsilon_{observed}$ and the objective is to deduce the horizontal stress σ_h producing this strain. As showed in Fig. 5, the same strain can be the consequence of several horizontal stresses, this is the

reason why an inverse model was developed to deduce the most probable horizontal stress σ_h.

3.1 Inverse model

For a strain measured by a VWE at a given location, Bayesian approach can be used to find in the database the probability of occurrence of each horizontal stress. The inverse model uses the following Bayes formula (Bayes 1763):

$$P\left(\sigma_{h_i}\middle|\varepsilon_{obs}\right) = \frac{P\left(\varepsilon_{obs}\middle|\sigma_{h_i}\right)\times P(\sigma_{h_i})}{\sum_{j=1}^{7} P\left(\varepsilon_{obs}\middle|\sigma_{h_j}\right)\times P(\sigma_{h_j})} \quad (2)$$

with ε_{obs} the strain measured by a VWE and σ_{h_i} the soil pressure (σ_h = {12, 13, 14, 15, 16, 17, 18}).

In addition to the intrinsic VWE error, the excitation amplitude of the wire has an effect on the measured resonant frequency. To account for the uncertainties related to this sensor accuracy, a confidence interval around the strain observed value ε_{obs} is created with [ε_{obs} (1 - 0.1 %); ε_{obs} (1 + 0.1 %)]. For each strain realization in the database, for each stress σ_i, the conditional probability $P(\varepsilon_{obs}|\sigma_{h_i})$ counts the number of occurrences in the considered interval. The occurrence probability of each $P(\sigma_{h_i})$ is considered as uniform (i.e. non informative law) that is to say $P(\sigma_{h_i}) = 1/7$.

For a given cross-section, several VWE may be placed. Consequently, several strain observations are considered for a given stress. In this case, Eq. 1 becomes:

$$\boldsymbol{P\left(\sigma_{h_i}\middle|\varepsilon_{obs\,1}, \varepsilon_{obs\,2}, \cdots, \varepsilon_{obs\,n}\right)} = \frac{\boldsymbol{P\left(\varepsilon_{obs\,1}, \varepsilon_{obs\,2}, \cdots, \varepsilon_{obs\,n}\middle|\sigma_{h_i}\right) * P(\sigma_{h_i})}}{\sum_{j=1}^{7} \boldsymbol{P\left(\varepsilon_{obs\,1}, \varepsilon_{obs\,2}, \cdots, \varepsilon_{obs\,n}\middle|\sigma_{h_j}\right) * P(\sigma_{h_j})}} \quad (3)$$

(Park and al. 2015) have studied the calculation error made when ignoring the correlation between the components of a system and showed in the case of the trellis design even the strongly correlated components have a minimal error in the optimization procedure. The article by (Baji and al. 2017) goes in the same direction with a negligible impact on the optimal maintenance strategy of a tunnel by ignoring the correlation between the components of a system. By considering the independence

285 of the input values, the calculation of the system is simplified, hence the use of this model. As strain observations can be considered independant, and it is possible to write:

$$P(\varepsilon_{obs_1}, \dots, \varepsilon_{obs_n}|\sigma_{h_i}) = P(\varepsilon_{obs_1}|\sigma_{h_i}) * \dots * P(\varepsilon_{obs_n}|\sigma_{h_i}) \quad (4)$$

290

in the following, $P(\sigma_{h_i}|\varepsilon_{obs_1}, \varepsilon_{obs_2}, \dots, \varepsilon_{obs_n})$ is denoted $P\%$.

3.2 Results

In a first phase, the inverse model gives results only for one strain observed by one VWE. For the VWE *P0e* at 0° extrados, (Fig. 2), the inverse model results are
295 presented in Fig. 6:

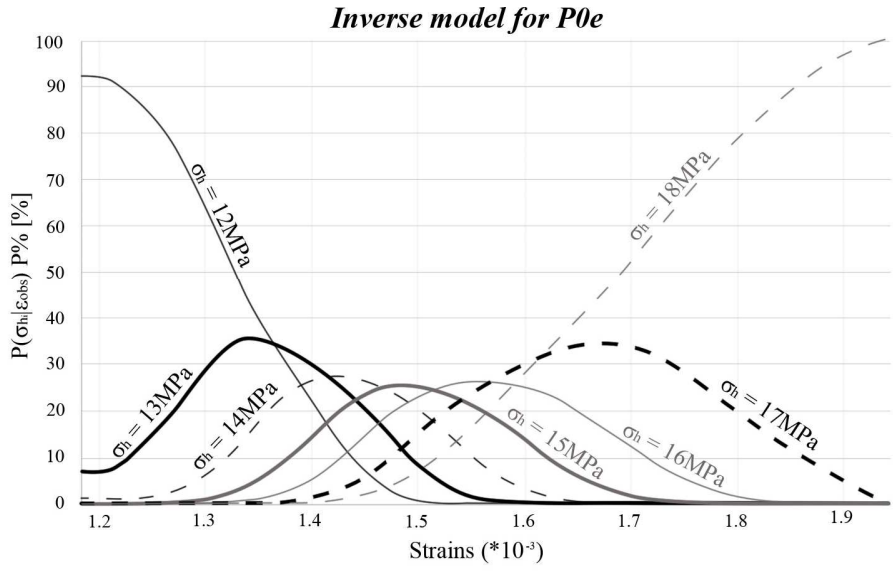

Fig. 6. Inverse model results for *P0e* strain observation (0° VWE extrados, Fig. 2).

This graph displays the evolution probability results of Eq. 2 (vertical axis) for different strain observations (horizontal axis) and each curve corresponds to one
300 stress.

For an observation $\varepsilon_{obs} = 1.2*10^{-3}$, the inverse model gives a probability ($P\%$) of *90 %* to have a stress $\sigma_h = 12$ MPa, $P\% = 9$ % for $\sigma_h = 13$ MPa and $P\% = 1$ % for $\sigma_h = 14$ MPa. For the other stresses (15, 16, 17 and 18 MPa), $P\% = 0$ %. Here, the inverse model is discriminant and allows us to find the most probable stress ($\sigma_h = 12$ MPa).

With a strain $\varepsilon_{obs} = 1.5*10^{-3}$, the highest probability of the inverse model gives $P\% = 27$ % for a stress $\sigma_h = 15$ MPa; the other probabilities are: $P\% = 21$ % for $\sigma_h = 16$ MPa and 14 MPa, $P\% = 12$ % for $\sigma_h = 17$ MPa, $P\% = 11$ % to have $\sigma_h = 13$ MPa, $P\% = 6$ % for $\sigma_h = 18$ MPa and $P\% = 2$ % to have $\sigma_h = 12$ MPa. In this second case, the inverse model is not discriminant.

Between $1.4*10^{-3}$ and $1.6*10^{-3}$, greatest probabilities are around *30 %*, which leads to overlapping curves of different stresses. The inverse model is not discriminant for only one strain observation and it is impossible to choose one unique horizontal stress for a cross-section in these cases.

In a second phase, the inverse model used several sensors (Fig. 7) for different positions (Fig. 8) when all strain observations are equal to $1.55*10^{-3}$.

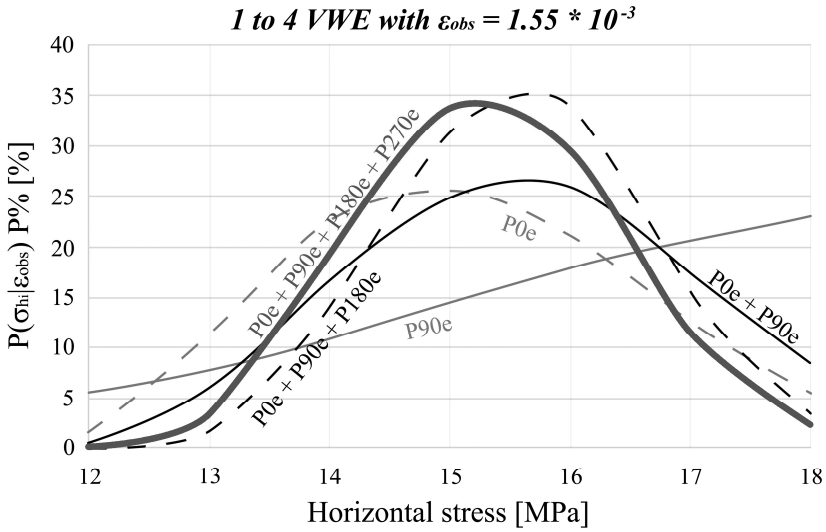

Fig. 7. Influence of the VWE numbers on the inverse model results.

Fig. 7 represents the probability results of Eq. 3 (vertical axis) versus each horizontal stress between 12 MPa to 18 MPa (horizontal axis). Each curve allows seeing the influence of the VWE numbers and the strain observations on the determination of the horizontal stress.

For just one sensor with a strain of $1.55*10^{-3}$, the sensor positioned at 0° extrados (point *P0e* on Fig. 2) gives a maximum pressure of *26 %* at 15 MPa and the point *P90e* (arch extrados) gives a maximum probability of *23 %* for 18 MPa. So the sensor location have an influence on the inverse model result. By combining information of two sensors at 0° and 90°, the best result is *27 %* for 16 MPa. While the sensor at 0° alone already gave a probability *P% = 26 %* for 15 MPa adding one sensor gives little more information. If there is three sensors at 0°, 90° and 180°, the best *P%* is equal to *34 %* for 16 MPa. Here, combining one more VWE extrados gives the best result of the inverse model. Finally adding one other sensor does not improve the previous solution.

Despite a relatively low probability, Fig. 7 shows that increasing the number of sensors provides better results. VWE positioned at kidneys (*P0e* and *P180e*) seem to give more information than sensors localized at arch and cross vault.

Adding sensors gives additional strain information, which logically improves the result of the likelihood function and thus improves the result of the inverse model. The vertical stress is constant and equal to 12.7 MPa, VWE placed near the vault and the cross vault will be influenced by this single value. For the horizontal stress, sensor locations near the kidneys will be more sensitive to this stress variations. In front of the most important information on the kidneys of the cell, the sensor combination at these locations increases the quality results more quickly than sensor locations in vault or cross vault.

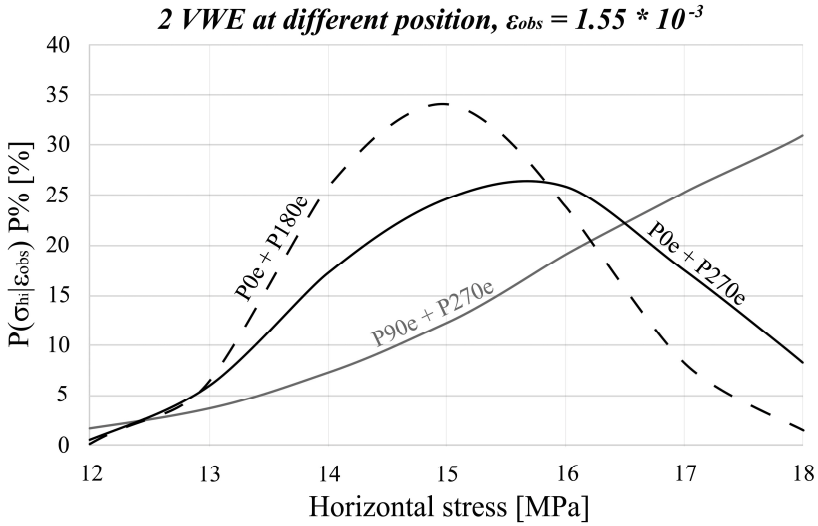

Fig. 8. Influence of two VWE positions on inverse model results.

Fig. 8 shows the variation of inverse model results according to the position of two sensors. As in the Fig. 7, the horizontal axis represents the horizontal stress and the vertical axis is the probability computed from Eq. 3. The duo arch (*P90e*) and cross vault sensors (*P270e*) provide the best probability of *31 %* for 18 MPa. This result is different to the other combinations. The couple 0°/270° gives *P% = 27 %* for 16 MPa and the best result is for the two kidneys with a probability of *34 %* to find a stress of 15 MPa.

This graph confirms the previous analysis that kidney sensors provide more information than arch and cross vault sensors.

4. Optimization for VWE numbers and locations

The purpose of the optimization is to find the best VWE location for a given number of sensors. So it consists in minimizing a fitness function taking into account:

- $\sigma_{h\,\%}$ the stress given by the inverse model as a function of β_i (β_i is the location β of the i^{th} VWE),
- the location of each sensor,

- $\sigma_{h\,dir}$ the stress computed from the numerical model that the inverse model should be able to find.

A genetic algorithm uses the fitness function to classify and select the best individual of a population.

4.1 Fitness function

Coupled with the inverse model, the fitness function helps us to solve the problem of optimizing the number and position of VWE. In order to select the "best" individual, the fitness function is:

$$\boldsymbol{f = (1-\alpha)\frac{\sum_1^7 P_i(\sigma_{h\,\%}-\sigma_{h\,dir})^2}{\sigma_{h\,dir}{}^2} + \alpha\frac{-\sum_1^7 P_i * \ln(P_i)}{-ln(P_\sigma)}} \quad (5)$$

The first term of the fitness function will therefore be able to compare the results of the inverse model $\sigma_{h\,\%}$ with the stress $\sigma_{h\,dir}$ of the DB from which the strains given as input parameters to the inverse model come.

The second term integrates the measurement of the dispersion of the results of the inverse model by considering all the horizontal stresses between 12 MPa and 18 MPa. Among the tools allowing to estimate the dispersion of a distribution, one finds in particular the Shannon entropy dispersion. Shannon's entropy (Shannon 2001) computes the disorder of a system. It is maximum when all the possibilities are a priori equiprobable. It is calculated using an information function inversely proportional to the occurrence probability of an observation. Entropy is used to evaluate the degree of certainty that one can have in data. This certainty is proportional to the dispersion of its belief mass on the judgment framework: i.e. data centred on a value will present more certainties than data interval including this value (representing more uncertainty in the evaluation).

In the second term denominator, $P_\sigma = {}^1/_7$ with "7" the discrete variable number σ_h, between 12 MPa and 18 MPa in a step of 1 MPa.

The coefficient α allows us to weight one or other of the two parts of the function. P_i is the probability of occurrence of each stress.

4.2 Genetic Algorithm

Genetic Algorithms (GA) are applied to sensor location optimization, according to the steps in Fig. 9. The algorithm explanation is presented with an example of five individuals with four couples of VWE intrados and extrados. Each individual is a
395 tunnel cross-section with four couples of sensors.

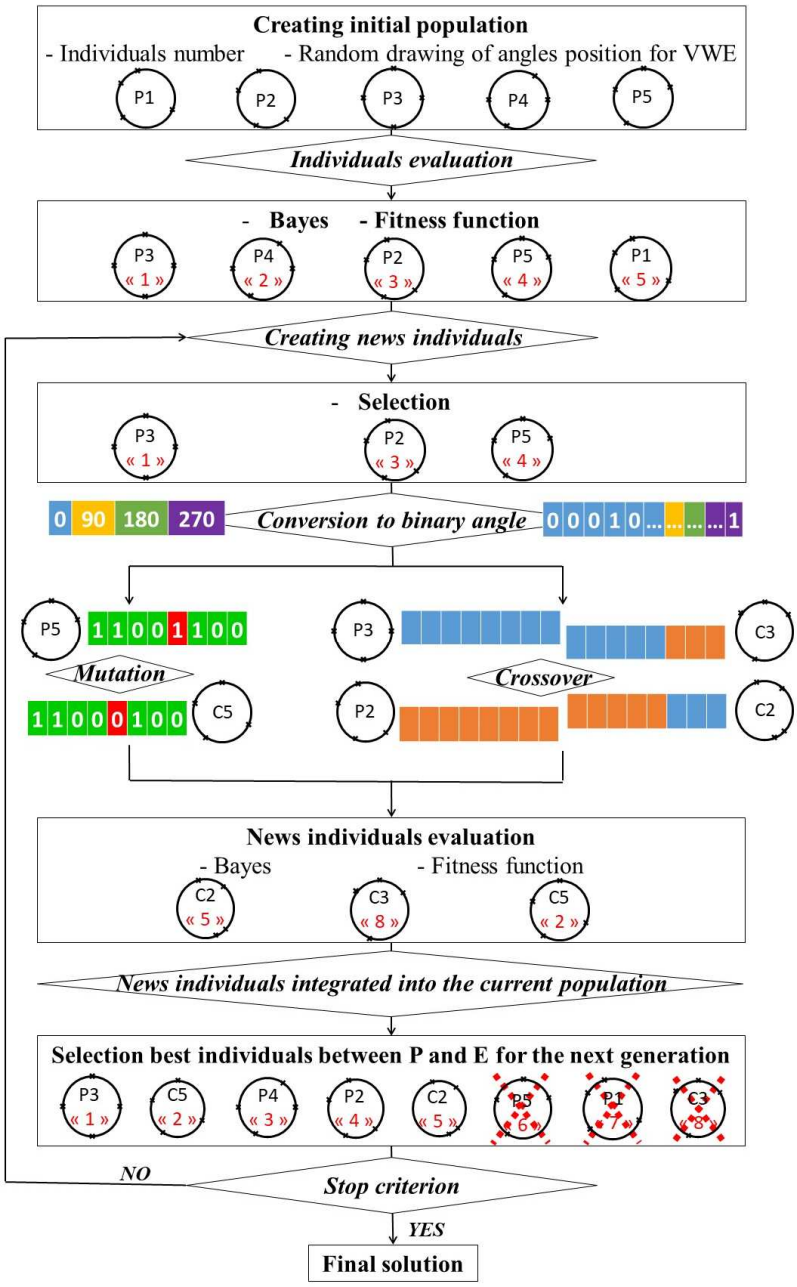

Fig. 9. Explanation of the different steps of GA allowing to obtain the best VWE locations in a cell cross-section from an initial population, for a given number of VWE.

In order to obtain the best individual (the one with the lowest result of the fitness function), the GA is a method to create new individuals from the best individuals of each generation.

The first step is to evaluate and rank individuals of this population according to their quality (results of inverse model and fitness function). This ranking appears in Fig. 9 by red number in quotation marks. Thus, *P3* individual is the best in the current population, ahead of *P4* individual which itself is of better quality than *P2* individual. Some of these individuals are selected to crossing-over and mutate to create new individuals and evolve the population. The number of selected individuals is unknown because it depends of individual numbers which are lower quality than a random value issue by a uniform law. The selection of certain individuals from the current population is done by the "roulette" method. The selected individuals see their angles converted into binary angles and all of them are glued to form chromosomes whose purpose will be to modify them.

The interest of creating new individuals from known individuals with this GA method is to keep the best solution while exploring the field of research to find individuals which can potentially be even better.

Several tests were carried out on the GA input parameters in order to make the optimal choice for the calculation. These input parameters are:

- The population size is the number of tunnel cross-sections with different VWE locations compared over a generation.
- The generation number corresponds to the number of fitness function tests on the entire population.
- The crossover probability is the percentage of individual selected in the population to create new individuals.
- The mutation probability is the percentage of individual selected in the population to create new individuals.

The next table presents the influence on the fitness function results for different input parameters.

Table 3

Different input parameters of GA for four couples of sensors intrados/extrados. P_c is the crossover probability and P_m is the mutation probability.

Test	*Population size*	*Generation number*	*Convergence generation*	*Pc*	*Pm*	*Position*				$f(*10^{-5})$
						VWE1	*VWE2*	*VWE3*	*VWE4*	
1	50	30	6	0.8	0.3	*0*	*102*	*171*	*280*	*1.46*
2	50	30	5	0.8	0.3	*4*	*95*	*171*	*280*	*1.49*
3	100	30	5	0.8	0.3	*0*	*102*	*171*	*280*	*1.46*
4	100	30	6	0.8	0.3	*91*	*171*	*280*	*354*	***1.26***
5	100	50	9	0.8	0.3	*0*	*102*	*171*	*280*	*1.46*
6	100	20	5	0.8	0.3	*4*	*95*	*171*	*280*	*1.49*
7	100	20	8	0.8	0.3	*91*	*171*	*280*	*354*	***1.26***
8	100	20	13	0.9	0.3	*91*	*171*	*280*	*354*	***1.26***
9	100	20	7	0.9	0.3	*91*	*171*	*280*	*354*	***1.26***
10	50	20	7	0.9	0.3	*91*	*171*	*280*	*354*	***1.26***
11	50	20	6	0.9	0.3	*4*	*95*	*171*	*280*	*1.49*
12	100	20	7	0.6	0.3	*91*	*171*	*280*	*354*	***1.26***
13	100	20	10	0.6	0.3	*0*	*102*	*171*	*280*	*1.46*

During these tests, the mutation probability P_m is always equal to 0.3 and the stop criterion matches to the number of generation. The first seven tests have a crossover probability P_c of 0.8. Tests *1* and *2* count the same generation numbers (50) and the same individual numbers per generation (30). A small population size combined with a low generation number provide sufficient exploration of the research space to obtain the convergence of *f*, but the result is not the minimum global of the function. With the same generation numbers (30) and double individual numbers (100), tests *3* and *4* gives different *f* result, but lower result appears. So the population size has an influence on the fitness function. The "bigger" is the population size, the best is the

fitness function result. On the other hand, larger is the population size, longer is the computation time. So it is crucial to look for an optimal population size.

The next steps shows the influence of the generation number to find the good fitness function as already found for test *4*. If a largest number of generations (50) does not give the best result of *f*, all tests converged to a single solution. With a low generation number (20) the fitness function does not give the best result all the time (tests *6* and *7*). 100 individuals out of 30 generations seems the best solution when the crossover probability is equal to 0.8.

To see the influence of the probability (P_c), different values were tested. The highest probability (0.9) allows a greater mixing of the population and more often gives the best result of the fitness function. Finally, for this probability, 20 generations is enough to converge towards the optimal solution. But if the population size is not large enough (50), *f* does not reach a minimum at each test.

As the calculation time is not significant, the chosen GA parameters are:

- Population size: 100,
- Generation numbers: 20,
- Crossover probability: $P_c = 0.9$,
- Mutation probability: $P_m = 0.3$.

GA are metaheuristic method, the result of which is a good optimization solution in a suitable calculation time. So the result of the fitness function it is not necessarily the minimum global. Despite the setting parameters presented previously, several identical tests converged to different solutions. So, the adopted solution for a generation numbers is presented Fig. 10. The first ten tests are performed by randomly drawing position angle of VWE for the 100 individuals of the population. At the end of each test, the ten best individuals are retained to represent $1/10^{th}$ of the initial population of the final test.

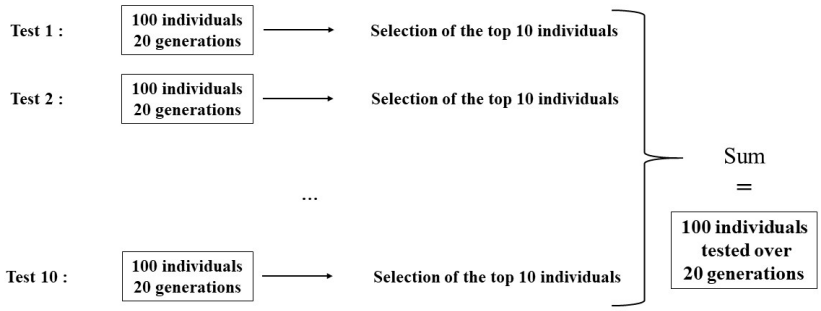

Fig. 10. Construction of the initial population for the latest test.

4.3 Results

Results are presented for different weights of the fitness function (Eq. 5) and for different number of VWE cages and different locations of these VWE. For the weighting coefficient, if $\alpha = 0$, only the difference to the target value $\sigma_{h\,target}$, in comparison to the inverse model result $\sigma_{h\,\%}$, is taken into account. When $\alpha = 1$, only the entropy of Shannon is considered. The other α values tested are *0.25* and *0.5*.

Table 4 and Fig. 11 present the results of the fitness function for 2 to 10 intrados and extrados VWE, with different α values.

Table 4

Fitness function results according to the VWE couple numbers.

α	VWE couple numbers								
	2	**3**	**4**	**5**	**6**	**7**	**8**	**9**	**10**
0	*0.009*	*0.003*	*0.001*	*0.000*	*0.000*	*0.000*	*0.000*	*0.000*	*0.000*
0.25	*0.481*	*0.221*	*0.087*	*0.044*	*0.019*	*0.009*	*0.004*	*0.002*	*0.001*
0.5	*0.948*	*0.477*	*0.209*	*0.079*	*0.034*	*0.014*	*0.007*	*0.003*	*0.002*
1	*1.883*	*0.855*	*0.411*	*0.173*	*0.064*	*0.026*	*0.010*	*0.004*	*0.002*

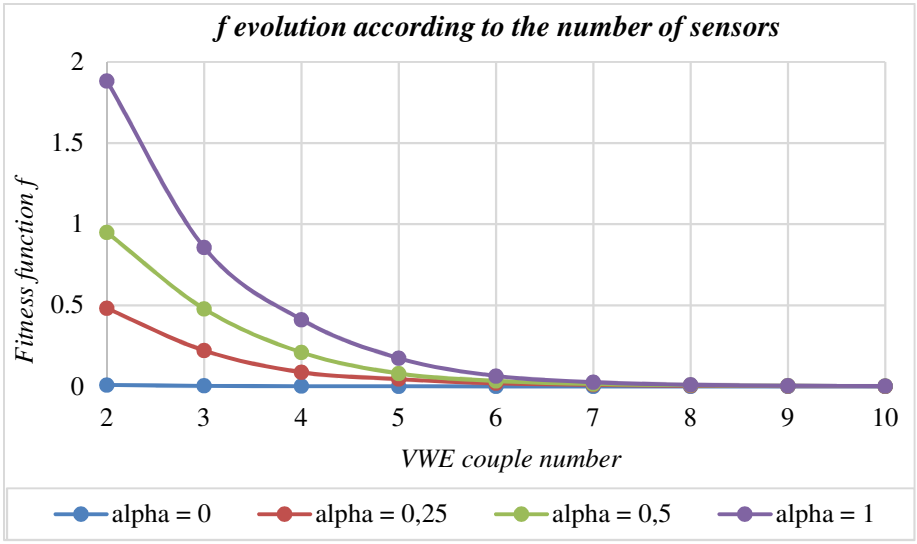

Fig. 11. Evolution of the fitness function for different α values.

- Influence of the weighting:

When $\alpha = 0$, $f = 0.001$ from 4 couples of VWE. In the same condition, $f = 0.087$ for $\alpha = 0.25$, $f = 0.209$ for $\alpha = 0.5$ and $f = 0.411$ for $\alpha = 1$. It is necessary to consider 5 couples of VWE to have $f < 1.10^{-2}$ for $\alpha = 0.25$ and $\alpha = 0.5$, and 6 couples of VWE when $\alpha = 1$. So, α value has an influence on the fitness function results f according to the VWE numbers. The weighting allowing to take into account the dispersion of the results of the inverse model increases the imprecision of the mathematical model. However, dispersion should be considered to account for uncertainties.

- Influence of the number of VWE cages:

Whatever the value of the weighting coefficient, the addition of a cage containing 2 VWE improves the result of the fitness function. Considering the uncertainties with a coefficient $\alpha = 0.25$, the addition of a couple of VWE improves, on average, the results of the fitness function of 24 %. This average improvement goes to 11 % when $\alpha = 0.5$.

To observe the position of 5 VWE couples on a cross-section, the results obtained by genetic algorithm are presented in Table 5.

Table 5

VWE positions and fitness function results in terms of α values.

α	VWE					f
	1	**2**	**3**	**4**	**5**	
0	22	53	205	325	352	$30*10^{-5}$
0.25	20	159	171	192	317	$4449*10^{-5}$
0.5	70	159	178	204	355	$7912*10^{-5}$
1	22	139	171	192	355	$17335*10^{-5}$

- Influence of the weighting:

When α increases, the fitness function increases and VWE positions vary.

- Influence of VWE cages location:

In addition to influencing the result of the fitness function, the measurement of the dispersion varies the optimization of VWE's positions. Except for VWE1 = 70° for $\alpha = 0.5$ and VWE2 = 53° for $\alpha = 0$, regardless of α value, all VWE are in the range of 90° around 0° (0° ± 45°, i.e. [315°, 45°]) and 180° (180° ± 45°, i.e. [135°, 225°]). This comfort results presented in part 3 (Fig. 7 and Fig. 8) that showed that VWE positioned at 0° or 180° seemed to provide more information than sensors localized in arch and cross vault.

For all results, VWE are generally located between [315°, 45°] and [135°, 225°]. With this observation, the best α value seems be *0.25* or *1*. By observing this result combined with the first result of f (Fig. 11 and Table 4) the best α value seems finally to be *0.25*.

Finally, the weighting have an influence of the inverse model results (Fig. 12).

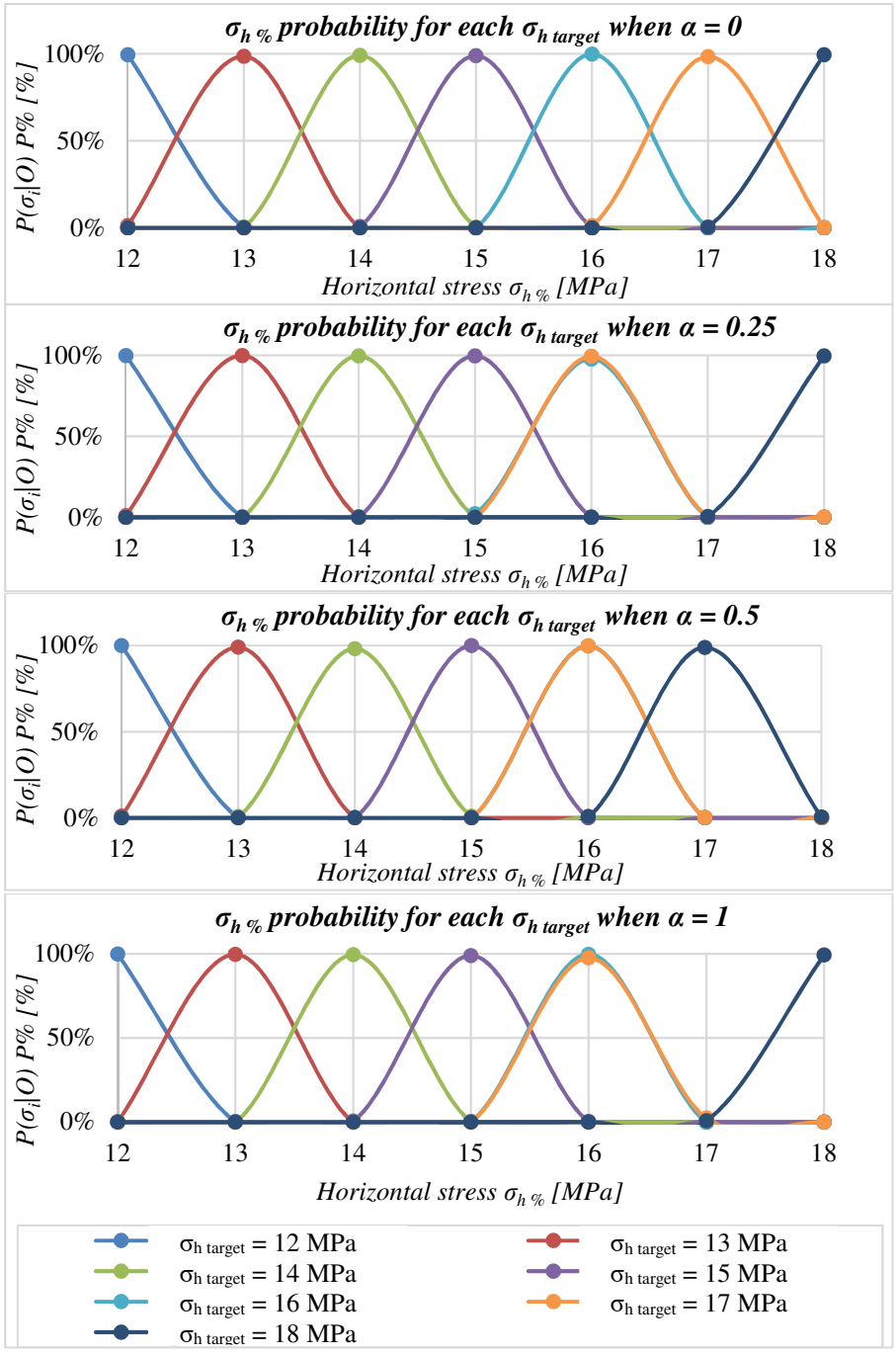

Fig. 12. Inverse model for each horizontal stress and different α for 5 VWE couples. For **a)** $\alpha = 0$, **b)** For $\alpha = 0.25$, **c)** For $\alpha = 0.5$, **d)** For $\alpha = 1$.

- Influence of the weighting:

In Fig. 12, each graph presents the result for one individual of 5 couples of VWE for all horizontal stresses. When $\alpha = 0$, the inverse model has about 100 % of good results for all $\sigma_{h\ target}$ (Fig. 12 a). When $\alpha \neq 0$, the inverse model is wrong for certain horizontal stresses like $\sigma_{h\ target}$ = 17 MPa for $\alpha = 0.25$ and $\alpha = 1$ (Fig. 12 b and d, orange curve) and for $\alpha = 0.5$ when $\sigma_{h\ target}$ = 17 MPa and $\sigma_{h\ target}$ = 18 MPa (Fig. 12 c, orange and dark blue curves).

The value of the dispersion influences the results. Indeed, the dispersion decreases the efficiency of the inverse model.

5. Conclusions

In order to optimize the location and the number of sensors in a tunnel cross-section, a three-step methodology has been developed. The first step consists in building a strain distribution database through a finite element analysis, taking into account uncertainties of the Young's modulus of the soil, intrinsic error of sensors and the angle error of sensors. The second step is to develop an inverse model using this database with Bayes theory, allowing us to estimate the most probable horizontal stress corresponding to a strain measured by a VWE. Finally, an optimization of the number and the position of sensors is proposed by using a Genetic Algorithm for various couples of orthoradial VWE. The results show that the dispersion of the inverse model plays a significant role on the fitness function and on the VWE locations. The choice of an optimal solution is a compromise between the inverse model results and the dispersion measurement. In our project, the best result seems to set up 5 VWE couples at locations in the ± 45° around 0° or 180°.

The solution presented in this article treats the problem in a discrete way – deformations at the VWE – whereas a continuous approach would allow treating the problem in its entirety – global deformation and highlighting of the interactions between close deformations. Consequently, the next step of this work is to optimize the VWE number and location to find the deformed tunnel cross-section and thus to verify that this deformed section does not prevent the handling of waste packages, as

required for the reversible management of Cigéo project. The fitness function will evolve to solve the optimization problem allowing to know the deformed shape. The uncertainty on the variable thickness concrete of the cell cross-section will be taken into account. The orientation (orthoradial or radial) and the number of VWE per cage will also be considered. Finally a 3D model can be set up in order to know the spacing between two consecutive sections.

Acknowledgements

This research is technically supported and funded by Andra (French national radioactive waste management agency).

References

Abdo M.A.-B. 2012. « Parametric Study of Using Only Static Response in Structural Damage Detection ». *Engineering Structures,* Vol. 34, p124-131.

Alexander W.R., and McKinley L. 2011. "Deep Geological Disposal of Radioactive Waste". Vol. 9. *Radioactivity in the Environment*. Elsevier.

Andra. 2005. "Evaluation de La Faisabilité Du Stockage Géologique En Formation Argileuse". Vol. Dossier Argile.

Ausiello G., Crescenzi P. and Protasi M. 1995. "Approximate Solution of NP Optimization Problems". Vol. 150, p1–55.

Aval K.J. and Abd Razak S. 2012. "A Review on the Implementation of Multiobjective Algorithms in Wireless Sensor Network". *World Applied Sciences Journal.* Vol. 19, n°6, p772–779.

Baji H., Li C.-Q., Scicluna S. and Dauth J. 2017. "Risk-Cost Optimised Maintenance Strategy for Tunnel Structures". *Tunnelling and Underground Space Technology,* Vol. 69, p72-84.

Bayes T. 1763. "An Essay towards Solving a Problem in the Doctrine of Chances". *Philosophical Transactions of the Royal Society of London.* Vol. 53, n°1, p370–418.

Bishop C.M. 1994. "Neural Networks and Their Applications". *Review of Scientific Instruments.* Vol. 65, n°6, p1803–1832.

Černỳ V. 1985. "Thermodynamical Approach to the Traveling Salesman Problem: An Efficient Simulation Algorithm". *Journal of Optimization Theory and Applications.* Vol. 45, n°1, p41–51.

Department of Business, Energy & Industrial Strategy. 2018. "Implementing Geological Disposal - Working with Communities. An Updated Framework for the Long-Term Management of Higher Activity Radioactive Waste".

Dinis da Gama C. 2004. "A Method for Continuous Monitoring of Tunnel Deformations during Construction and Service Phases". *In . Salzburg, Austria.*

Doebling S.W., Farrar C.R., Prime M.B. and Shevitz D.W. 1996. « Damage Identification and Health Monitoring of Structural and Mechanical Systems from Changes in Their Vibration Characteristics: A Literature Review ». Report LA--13070-MS, 249299.

Domingo-Perez F., Lazaro-Galilea J.L., Wieser A., Martin-Gorostiza E., Salido-Monzu D. and de la Llana A. 2016. "Sensor Placement Determination for Range-Difference Positioning Using Evolutionary Multi-Objective Optimization". *Expert Systems with Applications.* Vol. 47, p95–105.

Dorigo M. and Di Caro G. 1999. "Ant Colony Optimization: A New Meta-Heuristic". Proceeding, p1470-1477.

Dreyfus G., Martinez J.-M., Samuelides M., Gordon M.B., Badran F., Thiria S. and Hérault L. 2002. « Réseaux de neurones, méthodologie et applications. Chap 8 : Réseaux de neurones sans apprentissage pour l'optimisation ». Eyrolles.

Glover F. 1986. "Future Paths for Integer Programming and Links to Artificial Intelligence". *Computers & Operations Research.* Vol. 13, n°5, p533–549.

Goi Y. and Kim C.-W. 2017. « Anomaly detection of bridges under vehicle induced vibration by means of Bayesian inference ». *Fourth conference on smart monitoring assessment annd rehabilitation of civil structure*, Zurich, Switzerland.

Goldberg D.E. and Holland J.H. 1988. "Genetic Algorithms and Machine Learning". *Machine Learning*. Vol. 3, n°2, p95–99.

Greistorfer P. 2003. "A Tabu Scatter Search Metaheuristic for the Arc Routing Problem". *Computers & Industrial Engineering.* Vol. 44, n°2, p249–266.

Guan H. and Karbhari V.M. 2008. "Vabration-Based Structural Health Monitoring of Highway Bridges". *Report CA06-0081*. USA: University of California.

Guratzsch R.F. and Mahadevan S. 2006. "Sensor Placement Design for SHM under Uncertainty". *In Third European Workshop on Structural Health Monitoring, Granada, Spain*.

Guratzsch R.F. 2007. "Sensor Placement Optimization under Uncertainty for Structural Health Monitoring Systems of Hot Aerospace Structures". *PhD*. Nashville, Tennessee: Vanderbilt University.

Hammouche K. Diaf M. and Siarry P. 2010. "A Comparative Study of Various Meta-Heuristic Techniques Applied to the Multilevel Thresholding Problem". *Engineering Applications of Artificial Intelligence.* Vol. 23, n°5, p676–688.

Hao J-K, Galinier P. and Habib M. 1999. "Métaheuristiques Pour L'optimisation Combinatoire et L'affectation Sous Contraintes". *Revue D'intelligence Artificielle.* Vol. 13, n°2, p283–324.

Ihn JB. 2006. "Structural Health Monitoring. Overview & Aerospace Applications". *Presentation*.

Jacob S. 2006. "Le Dimensionnement Mécanique Des Tuyaux D'assainissement. Le Fascicule 70 Version 2003 et Les Cas de Pose Particuliers".

Jacquenot G. 2010. "Méthode Générique Pour L'optimisation D'agencement Géométrique et Fonctionnel". PhD Thesis, Ecole Centrale de Nantes (ECN).

Kennedy J. and Eberhart R. 1995. "Particle Swarm Optimization". p1942–1948.

Khoshahval F., Minuchehr H. and Zolfaghari A. 2011. "Performance Evaluation of PSO and GA in PWR Core Loading Pattern Optimization". *Nuclear Engineering and Design.* Vol. 241, n°3, p799–808.

Koh C.G. and Perry M.J. 2010. "Structural Identification and Damage Detection Using Genetic Algorithms". *Structures and Infrastructures Series*. Vol. 6. Boca Raton ; New york: CRC Press.

Kudva J.N., Munir N. and Tan P.W. 1992. "Damage Detection in Smart Structures Using Neural Networks and Finite-Element Analyses". *Smart Materials and Structures.* Vol. 1, n°2, p108.

Lifshitz J.M. and Rotem A. 1969. « Determination of Reinforcement Unbonding of Composites by a Vibration Technique ». *Journal of Composite Materials,* Vol. 3, n°3, p412-423.

Mei B. 2016. "Optimisation Des Couplages Magnéto-Mécaniques D'extensomètres À Corde Vibrante Pour Le Suivi Du Vieillissement de Constructions Stratégiques". *PhD*. Pierre et Marie Curie.

Moslem K. and Nafaspour R. 2002. "Structural Damage Detection by Genetic Algorithms". *AIAA Journal.* Vol. 40, n°7, p1395–1401.

Park C., Kim N.H. and Haftka R.T. 2015. "The effect of ignoring dependence between failure modes on evaluating system reliability". *Structural and Multidisciplinary Optimization,* Vol. 52, n° 2, p251–268.

Perry M.J., Koh C.G. and Choo Y.S. 2006. "Modified Genetic Algorithm Strategy for Structural Identification". *Computers & Structures.* Vol. 84, n°8–9, p529–540.Preis, Ami, and Avi Ostfeld. 2008. "Multiobjective Sensor Design for Water Distribution Systems Security." In *Water Distribution Systems Analysis Symposium 2006*, 1–17.

Ravi N.B., Chakraborty N. and Mahapatra D.R. 2016. "Simulation Based Optimization of Sensor Network for SHM of Complex Structures". *In 8th European Workhop On Structural Health Monitoring*. p1–7. Spain, Bilbao.

Rhim J. and Lee S.W. 1995. "A Neural Network Approach for Damage Detection and Identification of Structures". *Computational Mechanics.* Vol. 16, n°6, p437–443.

Rosin-Corre N., Noret C. and Bordes J.L. 2012. "L'auscultation Par Capteurs À Corde Vibrante, 80 Ans de Retour D'expérience". *In. Theme 2: Auscultation et suivi des ouvrages.* p1-15.

Rytter A. 1993. "Vibration Based Inspection of Civil Engineering Structures". *PhD.* Department of Building Technology and Structural Engineering, Aalborg University (Danemark).

Sbartaï Z.M., Laurens S., Elachachi S.M. and Payan C. 2012. "Concrete Properties Evaluation by Statistical Fusion of NDT Techniques". *Construction and Building Materials.* Vol. 37, p943–950.

Segretier W. 2013. "Approche Évolutionnaire et Agrégation de Variables: Application À La Prévision de Risques Hydrologiques". PhD Thesis, Antilles-Guyane.

Seleemah A.A., Abou-Rayan A. and Samy M. 2012. "A Neural Network Model for Damage Detection of El-Ferdan Bridge". *In. Fourth International Conference on Structural Stability and Dynamics*. Jaipur, India.

Shannon C.E. 2001. "A Mathematical Theory of Communication". Vol. 5, n°1, p3–55.

Spillman W.B., Huston D.R., Fuhr P.L. and Lord J.R. 1993. "Neural Network Damage Detection in a Bridge Element". *In Smart Structures and Materials 1993: Smart Sensing, Processing, and Instrumentation*. Vol. 1918, p288–300. International Society for Optics and Photonics.

Vanik M.W., Beck J.L. and Au SK. 2000. « Bayesian probabilistic approach to structural health monitoring ». *Journal of Engineering Mechanics,* Vol. 126, n° 7, p738–745.

Wrigley P.A., Wood P., Stewart P., Hall R. and Robertson D. 2019. "Module Layout Optimization Using a Genetic Algorithm in Light Water Modular Nuclear Reactor Power Plants". *Nuclear Engineering and Design.* Vol. 341, p100–111.

Wu Z.Y. and Walski T. 2006. "Multi Objective Optimization of Sensor Placement in Distribution Systems". *In 8th Annual Water Distribution Systems Analysis Symposium*. 11p. Cincinati, Ohio, USA.

Yan G., Sun H. and Büyüköztürk O. 2016. « Impact load identification for composite structures using Bayesian regularization and unscented Kalman filter ». *Structural Control and Health Monitoring,* Vol. 24, n° 5, 18p.

Zhang Y. and Yang W. 2012. « A New Damage Identification Strategy for SHM based on FBGs and Bayesian Model Updating Method ». In *ICF13*.

Zhou K. and Wu Z.Y. 2017. "Strain Gauge Placement Optimization for Structural Performance Assessment". *Engineering Structures.* Vol. 141, p184–197.